

Fermi National Accelerator Laboratory

FERMILAB-Conf-90/33-E
[E-741/CDF]

Asymmetry in Z^0 Decay at CDF*

The CDF Collaboration

presented by

Peter Hurst
University of Illinois
Urbana, Illinois 61801

January 1990

* Published in the proceedings of the 8th Topical Workshop on $p\bar{p}$ Collider Physics, Castiglione della Pescaia, Italy, September 1-5, 1989.



January 1990

Asymmetry in Z^0 Decay at CDF

The CDF Collaboration *

presented by Peter Hurst

The University of Illinois
Urbana, IL 61801, USA

Abstract

An analysis of the charge asymmetry in $p\bar{p} \rightarrow Z^0 \rightarrow e^+e^-$ events at CDF yields the preliminary value $\sin^2 \theta_W = 0.216 \pm 0.015$ (stat) ± 0.010 (sys).

1 Introduction

In the Standard Model of electroweak interactions [1], the neutral current is described as a mixture of the weak isospin and electromagnetic currents, with "mixing angle" θ_W , as shown below.

$$J_\mu^{NC} = J_\mu^{I_3} - \sin^2 \theta_W J_\mu^{EM}$$

The weak isospin component of the neutral current leads to a parity violating V - A form for the neutral current interaction, which is then slightly modified by the electromagnetic current. The vertex factor for the neutral interaction is given by

$$\frac{-ig}{\cos \theta_W} \gamma^\mu \frac{1}{2} (C_V^f - C_A^f \gamma^5)$$

where the vector and axial vector fermion couplings C_V^f and C_A^f are given by

$$C_V^f = T_f^3 - 2Q_f \sin^2 \theta_W \quad C_A^f = T_f^3$$

taking T_f^3 and Q_f to be the third component of weak isospin and the charge of the fermion, respectively. Due to the V - A form of the interaction, the Z^0 couples more strongly to left-handed fermions and right-handed antifermions. Using helicity and angular momentum conservation arguments similar to those used for charged current processes, one finds that in

* ANL - Brandeis - University of Chicago - Fermilab - INFN, Frascati - Harvard - University of Illinois - KEK - LBL - University of Pennsylvania - INFN, University and Scuola Normale Superiore of Pisa - Purdue - Rockefeller - Rutgers - Texas A&M - Tsukuba - University of Wisconsin

$f\bar{f} \rightarrow Z^0 \rightarrow f'\bar{f}'$ interactions the outgoing fermion (antifermion) is preferentially emitted in the direction of the incoming fermion (antifermion). This implies that there will be a charge asymmetry in the decay angular distribution of the Z^0 , and furthermore that the magnitude of this asymmetry depends on the values of the vector and axial vector couplings of the Z^0 . Since the vector and axial vector couplings themselves depend only on $\sin^2\theta_W$ and the (known) values of charge and isospin, one can infer a value for $\sin^2\theta_W$ from a measurement of the charge asymmetry in Z^0 decays. We propose, then, to determine $\sin^2\theta_W$ from a measurement of the dielectron angular distribution in $p\bar{p} \rightarrow Z^0 \rightarrow e^+e^-$ events at CDF.

At lowest order, both photon exchange and Z^0 exchange contribute to electron pair production in hadronic collisions; the Feynman diagrams for these processes are shown in Figure 1. A straightforward calculation based on these diagrams gives the cross section [2, 3]

$$\begin{aligned} \frac{d\hat{\sigma}}{d\cos\hat{\theta}} = N_C^f & \int_0^1 dx_a \int_0^1 dx_b \sum_q q(x_a, \hat{s}) \bar{q}(x_b, \hat{s}) \left\{ \frac{\pi\alpha^2 Q_q^2}{2\hat{s}} (1 + \cos^2\hat{\theta}) \right. \\ & - \frac{\alpha Q_q G_F M_Z^2 (\hat{s} - M_Z^2)}{2\sqrt{2}[(\hat{s} - M_Z^2)^2 + M_Z^2 \Gamma_Z^2]} [C_V^e C_V^q (1 + \cos^2\hat{\theta}) + 2C_A^e C_A^q \cos\hat{\theta}] \\ & + \frac{G_F^2 M_Z^4 \hat{s}}{16\pi[(\hat{s} - M_Z^2)^2 + M_Z^2 \Gamma_Z^2]} \\ & \left. \times [((C_V^e)^2 + (C_A^e)^2)((C_V^q)^2 + (C_A^q)^2)(1 + \cos^2\hat{\theta}) + 8C_V^e C_A^e C_V^q C_A^q \cos\hat{\theta}] \right\} \end{aligned}$$

where $\hat{\theta}$ is defined to be the angle between the outgoing electron and incoming quark (or outgoing positron and incoming antiquark) in the rest frame of the electron pair. Note that N_C^f is a color factor, $q(x_a, \hat{s})$ and $\bar{q}(x_b, \hat{s})$ are the quark distribution functions in the proton and antiproton, and the sum is over quark species. The first and third terms in the cross section are due to photon exchange and Z^0 exchange, respectively, while the second term arises from the quantum mechanical interference of these two subprocesses. Each term has a symmetric component proportional to $(1 + \cos^2\hat{\theta})$, and both the Z^0 and interference terms have antisymmetric components proportional to $\cos\hat{\theta}$. While the interference term is important in the charge asymmetries seen at lower energies, its contribution to the cross section near the Z peak is small (of order 1% of the total cross section). We wish to emphasize that the asymmetry seen in $p\bar{p} \rightarrow e^+e^-$ events is a feature of the Z^0 couplings to fermions, and is not merely an interference effect.

Finally, we note that when higher order effects are included, the precise definition of $\sin^2\theta_W$ changes. Values for $\sin^2\theta_W$ determined from different physical processes are not directly comparable until these higher order effects are taken into account. In particular, the value of $\sin^2\theta_W$ determined from the charge asymmetry is not yet directly comparable to the value determined by $1 - M_M^2/M_Z^2$.

2 Measuring $\cos\hat{\theta}$

The CDF detector has been described in detail elsewhere [4]. Here we briefly describe the detector components relevant to the asymmetry measurement. Two scintillator hodoscopes located on either side of the detector are used to identify inelastic events. A vertex time-projection chamber (VTPC) surrounds the interaction point and is used to measure the position of the event vertex. An axial wire drift chamber surrounds the VTPC and is used to measure the momentum of charged particles. Both of these tracking chambers are immersed in a 1.4 Tesla solenoidal magnetic field. Calorimeters extend from $-4.2 < \eta < 4.2$ and are organized into a projective tower geometry. In the central region ($|\eta| < 1.1$) the electromagnetic calorimeter consists of alternating layers of lead and scintillator while the hadronic calorimeter is composed of alternating layers of steel and scintillator. A gas proportional chamber is embedded in the central electromagnetic calorimeter near shower maximum to provide information about the shape and positions of electromagnetic showers. In the plug region ($1.1 < |\eta| < 2.4$) and forward region ($2.4 < |\eta| < 4.2$) the calorimeters consist of alternating layers of lead and gas proportional chambers in the electromagnetic calorimeters, and steel and gas proportional chambers in the hadronic calorimeters. For the asymmetry analysis, electron 4-vectors are defined by the position of the event vertex and the centroid and energy of an electromagnetic calorimeter cluster. Since $\cos\hat{\theta}$ is a charge dependent quantity, we must be able to measure the charge of at least one of the electrons. This requires that at least one of the electrons leave a well reconstructed track in the drift chamber.

There are a number of other factors which are of importance in measuring $\cos\hat{\theta}$. First, $\hat{\theta}$ is defined by the quark and antiquark directions. In practice, we know the directions of the protons and antiprotons only; we assume that the initial quark is moving in the proton direction and the initial antiquark is moving in the antiproton direction. While this is always true for interactions involving valence quarks, we will be wrong half the time for interactions in which both quarks come from the Fermi sea. Since we mismeasure the sign of $\cos\hat{\theta}$ for half of the sea-sea interactions, we find that the sea-sea interactions will give a symmetric “background” contribution to the asymmetry.

Next, we find that due to QCD effects such as initial state gluon bremsstrahlung, the lepton pairs are emitted with varying amounts of transverse momentum, P_T . When a lepton pair is produced with non-zero P_T , the directions of the incident quarks in the rest frame of the lepton pair are not completely determined. The quarks can only be said to be travelling in approximately the direction of the proton or antiproton, and this approximation gets worse as P_T increases. Since the initial quark directions are ill-defined, $\cos\hat{\theta}$ can no longer be precisely measured. We will use the method of Collins and Soper [5] to redefine $\cos\theta$ in a consistent, though P_T dependent, way. We thus expect that the $\cos\hat{\theta}$ distribution will be smeared somewhat by the high P_T events.

Finally, we note that if we simply exchange the identities of the electron and positron in any dielectron event, the event topology remains unchanged while $\cos\hat{\theta}$ changes sign. If the detector acceptance depends only on the event topology and not on the charges of the

electrons, then the acceptance must be independent of the sign of $\cos \hat{\theta}$, and must therefore be symmetric with respect to $\cos \hat{\theta}$.

3 Data Sample and Results

Using data corresponding to an integrated luminosity of 4.6pb^{-1} , we have extracted a dielectron sample using the following requirements:

- each event must satisfy the CDF diphoton trigger. The diphoton trigger requires 2 electromagnetic clusters, each having $E_T > 10$ GeV and the ratio of total E_T to electromagnetic E_T , $E_T/E_T^{\text{em}} < 1.125$.
- calorimeter clusters with $|\eta| < 0.9$ must have an associated track from the trigger fast track processor with $P_T > 6$ GeV
- the invariant mass of the electron pair must be greater than 50 GeV
- all events were hand-scanned to remove obvious background events.

This process produced a sample containing 597 events. For the asymmetry measurement, we applied the following additional cuts to this dielectron sample:

- $E_T > 15$ GeV for both electrons
- one central ($|\eta| < 1.0$) electron cluster with associated 3-D track and ratio of cluster energy to track momentum, $E/P < 2.0$.
- lateral and longitudinal shower profiles consistent with an electron shower
- the cluster centroid located away from calorimeter edges

A total of 314 events satisfy these requirements. A plot of dielectron invariant mass for these events is shown in Figure 2. For the final asymmetry measurement we use only the 272 events in the range $76 \text{ GeV} < M_{ee} < 106 \text{ GeV}$.

A plot of $dn/d\cos\hat{\theta}$ for events satisfying the above electron quality and mass cuts is shown in Figure 3. We observe that there are more events with positive values of $\cos\hat{\theta}$ than negative values, as expected. Further, the $dn/d\cos\hat{\theta}$ distribution has the parabolic shape predicted by the cross section calculated previously. Finally, we note that the geometrical acceptance of the CDF detector falls off as $|\cos\hat{\theta}|$ approaches 1.0, and so we see a reduced number of events in the outermost bins of Figure 3.

We can determine $\sin^2\theta_W$ by fitting the data to the theoretical prediction for the cross section given above. We use a negative log likelihood method and fit the data event by event. Note that the fit has been constructed in such a way that the minimization process is independent of acceptance if the acceptance is symmetric with respect to $\cos\hat{\theta}$. We assume that the acceptance is charge independent, which implies that the acceptance is symmetric with respect to $\cos\hat{\theta}$, and so we fit the data without making acceptance corrections. Finally,

we must choose a set of proton structure functions in order to obtain the proper u quark to d quark and valence to sea ratios. Using EHLQ Set 1 structure functions, we obtain a preliminary value of $\sin^2 \theta_W = 0.216 \pm 0.015$ where the quoted error is purely statistical.

There are a number of systematic effects which can affect the measurement of $\sin^2 \theta_W$. Since we are using calorimeter cluster energies and centroids to measure the electron 4-vectors, the accuracy with which we can determine $\cos \hat{\theta}$ will be determined by the finite position and energy resolution of the detector. We find from Monte Carlo studies that our measurement of $\sin^2 \theta_W$ is insensitive to detector resolutions. We also find that we are insensitive to small (5%) energy scale differences between calorimeter elements.

Charge dependent biases in the data are expected to be small. Our initial event selection is based on the diphoton trigger, which is charge independent, and the trigger fast track processor. When we correct the tracking information for false curvatures offline, and then make an effective track P_T cut (the E/P cut in conjunction with the E_T cut), we remove any charge-related bias due to the trigger processor track cut. Residual biases due to this effective P_T cut are expected to be small because 1) the false curvatures which remain after the tracking corrections are made are small, and 2) the cut is made in a sparsely populated region of the Jacobian P_T distribution, and hence can affect few events. Away from the P_T cut, we need only to be able to distinguish the charges. We find that there are no same-sign central-central Z^0 events in our final sample, and no peak at the J/ψ or Υ mass in the same-sign dimuon mass distribution. We believe, then, that we are able to reliably distinguish positively charged particles from negative particles.

From the dielectron invariant mass distribution shown in Figure 2 we estimate that there is less than 5% background under the peak between 76 and 106 GeV. If we assume a 5% background symmetric in $\cos \hat{\theta}$, we find that our value of $\sin^2 \theta_W$ is reduced by 0.002. We therefore assign a systematic error of 0.002 to our results to represent the effect of background in our data sample.

Recall that $\cos \hat{\theta}$ is ill-defined in events having large P_T , and so we expect the $\cos \hat{\theta}$ distribution to be smeared somewhat by the high P_T events. We use the ISAJET [6] Monte Carlo to estimate the effect of this smearing on our result. We have generated two large samples, one in which the P_T is restricted to be below 5 GeV, and in which we believe the smearing to be negligible, and one in which the Monte Carlo P_T spectrum has been tuned to reproduce the P_T spectrum seen in the CDF data. We find that the $\sin^2 \theta_W$ values derived from these two samples differ by approximately 0.0005. The statistical error on the Monte Carlo measurements, however, is of order 0.001. We therefore assign a conservative systematic error of 0.001 to our result due to smearing in high P_T events.

Finally, we recall that the angular distribution depends on the proton structure functions in two different ways. First, u-type quarks and d-type quarks couple differently to the Z^0 , and so our result will depend on the u to d ratio in the proton. Second, sea-sea interactions produce a symmetric “background” to the valence quark interactions which we must take into account. Now, there is some uncertainty in the structure functions, especially at low x , where most Z^0 production takes place. We estimate the systematic error due to this uncertainty by fitting our data with several different structure function parametrizations

Log-Likelihood Fit Results 1988-1989 Data CDF PRELIMINARY		
Parametrization	$\sin^2 \theta_W$	Error
EHLQ 1	0.216	0.015
EHLQ 2	0.216	0.015
DO 1	0.216	0.015
DO 2	0.200	0.023
DFLM 1	0.217	0.014
DFLM 2	0.216	0.015
DFLM 3	0.216	0.015
MRS 1	0.215	0.016
MRS 2	0.222	0.013

Table 1: Fit results for various structure function parametrizations

[7]. The results are shown in Table 3. We find that there is a spread in the $\sin^2 \theta_W$ values of approximately 0.02, and so we assign a conservative systematic error of 0.01 to our result to represent the uncertainty in the proton structure functions.

4 Conclusion

Using the charge asymmetry in $p\bar{p} \rightarrow Z^0 \rightarrow e^+e^-$ events, CDF has obtained the preliminary value $\sin^2 \theta_W = 0.216 \pm 0.015(\text{stat}) \pm 0.010(\text{sys})$, where the systematic error is dominated by the uncertainty in the structure functions. This value agrees with the value obtained previously by UA1, $\sin^2 \theta_W = 0.24_{-0.04}^{+0.05}$ [8], from the asymmetry in 33 selected $Z^0 \rightarrow e^+e^-$ and $Z^0 \rightarrow \mu^+\mu^-$ events. No electroweak radiative corrections have been applied, and so it is inappropriate at this time to compare our value with values obtained from other physical processes.

References

- [1] S.L. Glashow, Nucl. Phys.B **22**, 579 (1961);
S. Weinberg, Phys. Rev. Lett. **19**, 1264 (1967);
A. Salam, in *Elementary Particle Theory*, edited by N. Svartholm (Almquist and Wiskell, Stockholm, 1968), p.367
- [2] M. Böhm, W. Hollik, Nucl. Phys. **B 204**, 45 (1982)
- [3] V. D. Barger and R. J. N. Phillips, *Collider Physics* (Addison-Wesley, Reading, Massachusetts, 1987)

- [4] F. Abe et. al., Nucl. Inst. and Meth. **A 271**, 387 (1988)
- [5] J.C. Collins and D.E. Soper, Phys. Rev. **D 16**, 2219 (1977)
- [6] F. Paige and S.D. Protopopescu, BNL Report No. BNL 38034, 1986 (unpublished)
- [7] E. Eichten, I. Hinchliffe, K. Lane, and C. Quigg, Rev. Mod. Phys. **56**, 579 (1984);
D.W. Duke and J.F. Owens, Phys. Rev. **D 30**, 49 (1984);
M. Diemoz, F. Ferroni, E. Longo, and G. Martinelli, Z. Phys. **C 39**, 21 (1988);
A. D. Martin, R. G. Roberts, and W. J. Stirling, Phys. Rev. **D 37**, 1161 (1988)
- [8] T. Müller, Fortschr. Phys. **37**, 339 (1989)

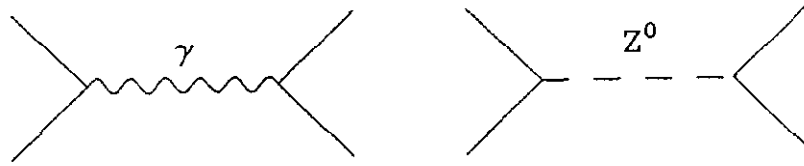


Figure 1: Lowest order Feynman diagrams for $p\bar{p} \rightarrow e^+e^-$

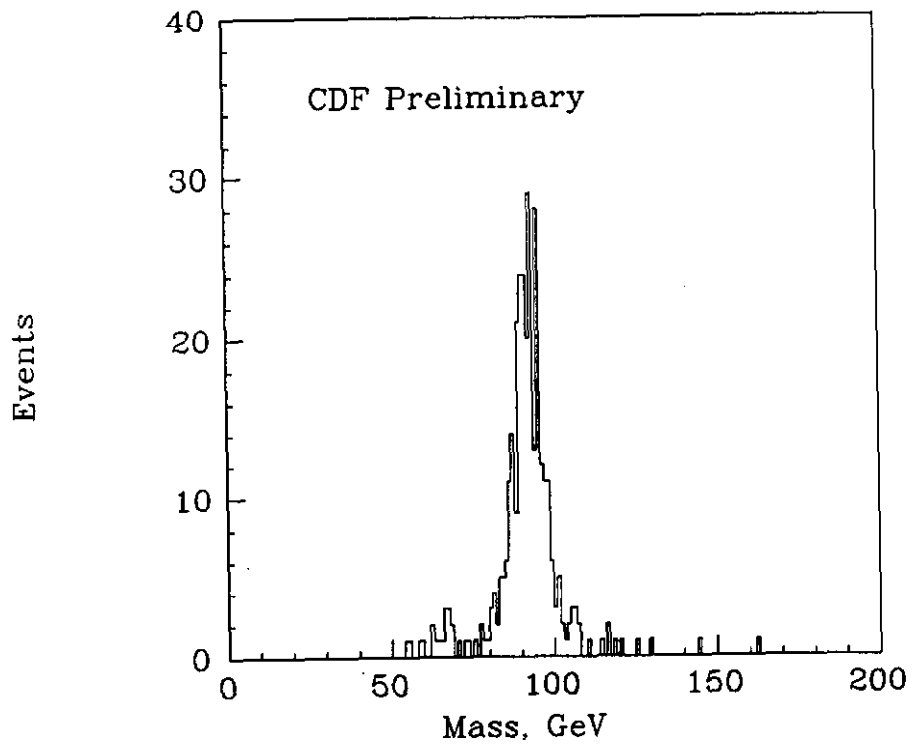


Figure 2: Dielectron invariant mass

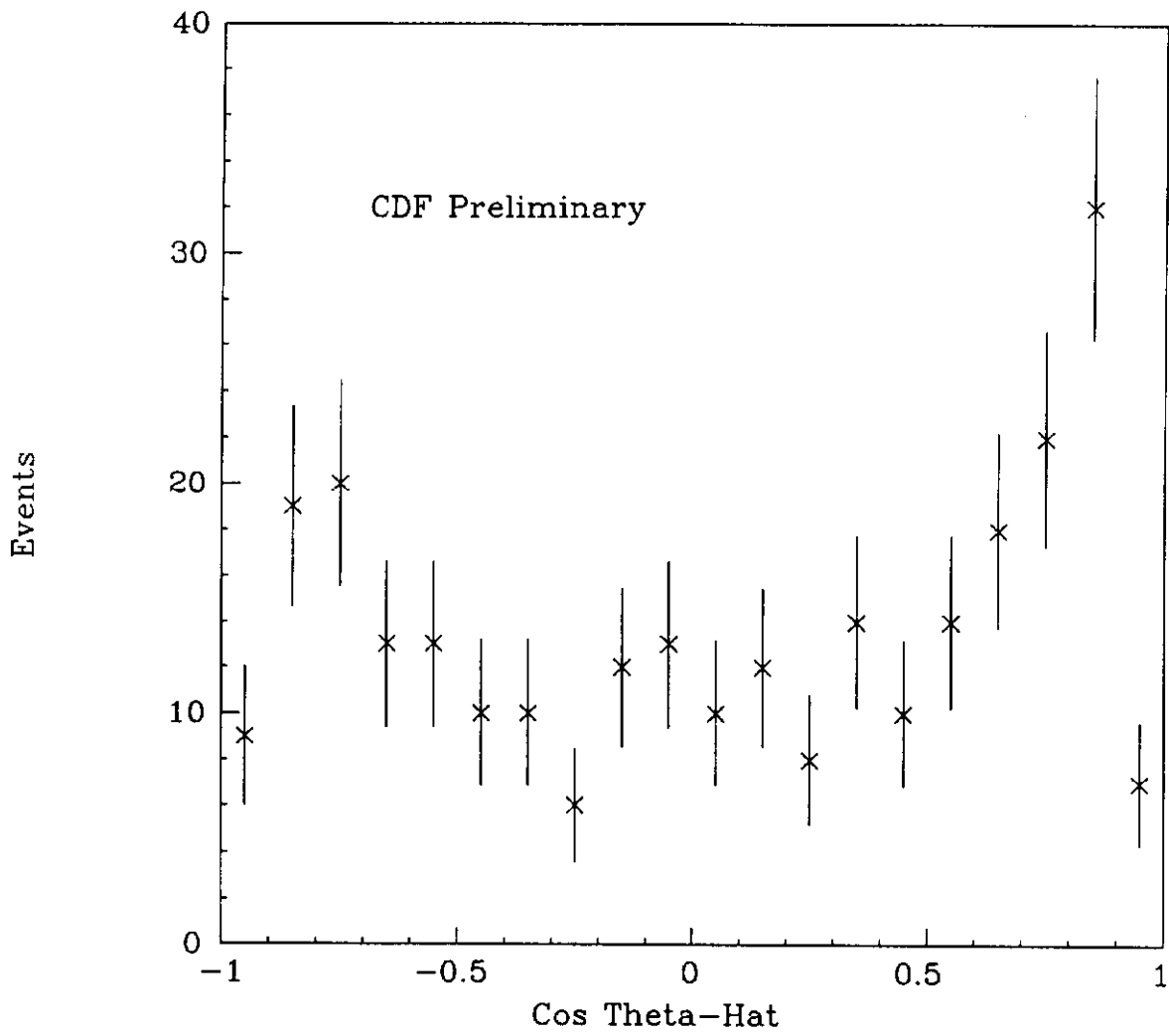


Figure 3: Uncorrected $\cos \hat{\theta}$ distribution